Evaluation of chloride contamination in concrete using electromagnetic non-destructive testing methods

Xavier Derobert, Jean-François Lataste, Jean-Paul Balayssac, S. Laurens

Evaluation of chloride contamination in concrete using electromagnetic non-destructive testing methods

Xavier Dérobert[1]*, J.F. Lataste[2], J.-P. Balayssac[3], S. Laurens[3]

[1]*LUNAM université, IFSTTAR, CS4, 44344 Bouguenais, France*

[2]*University of Bordeaux, I2M, 33 400 Talence, France*

[3]*LMDC, INSA/UPS Génie Civil, 135 Avenue de Rangueil, 31077 Toulouse cedex 04 France*

Corresponding author: *xavier.derobert@ifsttar.fr*

Ifsttar, route de Bouaye, CS4, 44344 Bouguenais, France

Tel: +33 (0)2 40 84 59 11 Fax: +33 (0)2 40 84 59 97

Abstract

We present the results of the sensitivity of some electromagnetic non-destructive testing (NDT) methods to chloride contamination. The NDT methods are resistivity, using a quadripole probe, capacitive technique, with few sets of electrodes, and radar technique, using different bistatic configurations. A laboratory study was carried out involving three different concretes with different water to cement ratios. The concretes were conditioned with different degrees of NaCl saturation by means of three solutions containing 0 g/L, 30 g/l or 120 g/l. The solution was homogenized in the concrete by using a specific procedure. Results show that the EM techniques are very sensitive to the chloride content and saturation rate and, on a second level, to the porosity. Multi-linear regression processing was performed to estimate the level of sensitivity of the NDT measurements to the three indicators. Values of ten ND observables are presented and discussed. At last, the uncertainties of the regression models are studied on a real structure in a tidal zone.

Keywords: radar, resistivity, capacitance, humidity, concrete, chloride, measurement

uncertainty

1. Introduction

Chloride-induced corrosion is one of the major causes of degradation of reinforced concrete structures, considering marine exposure conditions or the extensive use of de-icing salts in many countries. Reliable assessment of existing structures is based on the knowledge of chloride concentration values, as the residual service life is estimated from the time required to reach the chloride threshold value at the depth of the reinforcement [1-3].

Although the destructive characterization of chloride content is now fully applied all over the world, it is widely recognized that the procedure is cumbersome and requires a lot of time, and that any non-destructive technique able to provide this information would bring an appreciable improvement to the assessment methodologies [4]. The complexity of the diagnosis is partially due to the multiple influences included during the measurement and the inversion process, all of which act as sources of uncertainty in the diagnosis. Generally, to assess an indicator (e.g. chloride content), all other properties are assumed to be constant. This assumption is either justified – and the diagnosis is accurate – or false – but the approach is still used for lack of another solution. The latter case is the more frequent, which is why improvements to NDT methods and interpretation methodology are long overdue.

Numerous studies have shown the great potential of electromagnetic (EM) techniques, including electrical ones, for the evaluation of concrete durability indicators, such as water content, chloride content and, to a lesser extent, porosity [5-12]. These studies, performed on different concrete mixes, have shown the high level of sensitivity of the EM observables (from conductivity to relative permittivity at radar frequencies) to these

durability indicators.

A national project gathering six academic partners and six industrials, the “Strategy of non-destructive evaluation for the monitoring of concrete structures” (SENSO) project, aimed to propose a methodology for the non-destructive evaluation of some indicators related to the durability of concrete by means of a combination of numerous non-destructive testing (NDT) methods, including electrical, EM and ultra-sonic (US) techniques [13]. For each indicator, the objectives were to evaluate its value (average and degree of variability) and to estimate the degree of reliability of this evaluation. An important experimental study was carried out on controlled samples (homogeneous regarding the variation of indicators inside the samples) and a large database was built up and explored to draw relationships between NDT measurements and indicators [13-16]. Saturation rate, porosity, carbonation depth and chloride ingress were the indicators addressed for 8 different concrete compositions, and were investigated with more than 11 ND methods.

Within that framework, a specific experimental programme was dedicated to chloride content, and the objective of this paper is to present the results of that study. Laboratory experiments were carried out on three different concretes using three saturation degrees of solutions involving two concentrations of NaCl (30 and 120 g/l). The quantities of total chloride were assessed by chemical titration and NDT measurements were performed at the same time. As US techniques showed very low sensitivity to chloride content, only the electrical and EM techniques are presented and discussed below.

In this paper, the objective of the first study is to determine multilinear regressions between ND measurements and specific indicators: saturation rate, porosity and chloride content, for various depths, on controlled concrete samples. The second part

studies the use of these regressions to estimate chloride content, also addressing the question of uncertainty at the levels of methods and models. Then, the last part is devoted to their implementation on a real site in a tidal zone. The discussion only focuses on the choice of techniques for chloride contamination diagnosis here, and on the uncertainty levels.

2. Experimental design

2.1. Preparation and conditioning of concretes

Focusing on chlorides, three concretes were made using the same cement (CEMI 52.5 N from Calcia) and the same nature of aggregates (round siliceous) from the River Garonne. The details are presented in Table 1, keeping the same references as those used in the SENSO project [13]. For each mix, 11 slabs (50x25x12 cm) were cast and water cured for 28 days. Three of these slabs were devoted to assessment of the porosity, the compressive strength and the characterization of the Young's modulus**.**

Table 1. *Concrete characteristics*

Aggregates	**Round Siliceous (0/20 mm)**		
Reference	**G1**	**G3**	**G8**
W/C	0.30	0.55	0.80
Cement (kg/m^3)	405*	370	240
28 day strengh (MPa)	72.9	43.8	20.2
Density (kg/m^3)	2541	2457	2405
Porosity (%)	12.5	15.5	18.1

* addition of 45 kg/m^3 of silica fume

The other 8 slabs were contaminated with different concentrations of chlorides. After drying at 80°C until their weight became constant, 4 slabs were contaminated by absorbing a solution of water containing 30 g/l of NaCl (CL-1) at three different saturation degrees (one slab at 40%, one slab at 80% and two slabs at 100%). The other

4 slabs were contaminated with a solution of water containing 120 g/l of NaCl (CL-2) in the same conditions of saturation. After absorbing the quantity of salt water corresponding to a given saturation degree, each slab was sealed in a polyethylene sheet and adhesive aluminium foil.

They were then placed in an oven at 80°C for three months to homogenize the interstitial solution. Before the contamination with chlorides, the slabs were conditioned at 5 different levels of saturation (0, 40%, 60%, 80% and 100% of tap water) and tested with NDT methods in the same conditions as for chloride contamination (CL-0). Thus it was possible to compare the effect of chloride contamination on NDT measurements on the sample samples. Table A1, in appendix, summarizes the saturation rate for all the concretes, the porosity (measured on only 1 slab) and the total chloride content in percentage weight of dry concrete, assessed by chemical titration at different depths (5, 10, 15 and 20 mm). It can be seen that there was no significant chloride gradient over the depth investigated by titration.

2.2. NDT measurements

Radar technique

The radar techniques developed in the framework of this study relied on commercial ground-penetrating radar (GPR) systems, using SIR-3000 systems from Geophysical Survey Systems Inc. (GSSI®) and two separate ground-coupled 1.5 GHz antennas. Two approaches were employed. One of them used four offsets (transmitter-receiver distance), ranging from 7 to 14 cm, with an absorbing sponge placed between the transmitter and the receiver, in order to measure the direct wave in the medium without distortion due to the direct air wave [16]. Few observables were studied with this

configuration: the velocity, the corresponding relative permittivity and the attenuation from the direct wave, and the arrival time for the largest offset. For the attenuation, the observable studied corresponded to the slope coefficient of the logarithm of the amplitudes.

The second approach, with one standard 1.5 GHz antenna, directly measured the peak-to-peak amplitude of the direct wave in the medium [6-7]. This amplitude was normalized to the peak-to-peak amplitude of the signal in air. For both configurations, the coupled thickness of the medium, in the near vicinity of a GPR antenna which interacts with it, can be estimated at 8-10 cm.

Capacitive technique

This technique, and the corresponding sensor, was designed by the network of laboratories of the Ministry of Ecology, Sustainable Development and Energy (France) and tested in reinforced concrete structures [16-18]. The principle of the capacitive technique is to measure the resonance frequency of an oscillating circuit (around 30-35 MHz) between several electrodes lying on the upper face of the concrete slab. A calibration allows the concrete relative permittivity ε'_r to be obtained, which is mainly related to the water content and the mixture components. The volume investigated depends on the geometry of the electrodes (coupled depth of roughly 1-2 cm for medium sized electrodes – ME – and 6-8 cm for large electrodes – GE).

Resistivity technique

The technique tested in this study used a four-probe square device that injects electrical current between two lateral probes and measures the potential difference between the

142 other two probes [18-20]. The apparent resistivity is deduced from the ratio of the
143 potential to the intensity, according to the geometrical characteristics. Measurements,
144 with two spacings (5 and 10 cm), were performed for two orthogonal directions of
145 electrical current injection and then averaged, for coupling thicknesses of about 3 and 6
146 cm respectively. For an accurate analysis, given the wide range of variation of resistivity
147 between concretes in different states of moisture and chloride content, it is necessary to
148 study the resistivity in its logarithmic form (Log(Res)).
149 In the following text, the term “observable” will be used as a generic term for all the ND
150 studied observables (Table A2, in appendix).
151

152 ## *3.* Laboratory results

153 The first campaigns in the SENSO project showed that most of the NDT techniques
154 tended to give results that varied linearly with the indicators. As the EM techniques are
155 sensitive to both water and chloride content, and indirectly to the porosity, some
156 regression functions to one indicator can only be proposed when the other two are
157 constant. The data were processed to fit a multi-linear regression (3-parameter) function
158 on the three indicators, under the hypothesis of averaged values without depth gradient.
159 Equation 1, for the GPR velocity, is presented as a model equation:

160 $$Velocity_{GPR} = a \cdot Poro + b \cdot S_r + c \cdot Cl^- + d \quad (1)$$

161 where *Poro*, S_r and Cl^- correspond to the porosity, the saturation rate and the chloride
162 content, respectively, and *a*, *b*, *c* and *d* to the multi-linear regression coefficients.
163 Some ND observables require specific adaptation, such as the GPR signal attenuation
164 and the resistivity measurements. Concerning the electrical resistivity, for concrete, as
165 for porous materials, the empirical Archie’s law is used and expressed as:

166 $$R = a \cdot Poro^{-m} \cdot R_w \cdot S_r^{-n} \quad (2)$$

167 where the porosity, *Poro*, and the saturation, *Sr*, are clearly factors influencing the
168 resistivity *R*, and where the influence of chloride is represented through the interstitial
169 fluid resistivity (R_w). Expressed in logarithmic terms, the law becomes:

170 $$Log\ R = Log\ a - m \cdot Log\ Poro + Log\ R_w - n \cdot Log\ S_r \quad (3)$$

171 where, considering the range of variation for porosity (12 to 18%) and saturation (40 to
172 100%), we can accept that Log *Poro* and Log S_r are proportional to *Poro* and S_r,
173 respectively. For Cl^-, a link with R_w also exists [21-22]. Finally, the linear regression
174 approach chosen (Eq. 1), is very comparable with the well known Archie's law for
175 resistivity; and *a*, *b*, *c* and *d* are indicators of *a*, *m*, and *n* of the Archie's law. Similarly,
176 as the GPR attenuation is exponential through its propagation in a medium, a
177 logarithmic approach enables the model equation shown in Eq. 1 to be used.
178 Figure 1 presents, through the example of the GPR velocity, the dispersion of the
179 measurements when only one indicator is considered (Fig.1a-b), or when two or the
180 three indicators are considered through the modelling of the velocity using the muli-
181 linear regression coefficients from Equation 1 in Figures 1c-d. We note that the
182 determination coefficient R^2 is not significant (< 0.7) for the simple regressions (Figs
183 1a-1b) but it increases notably to 0.83 for a 2-parameter regression on S_r and Cl^-
184 (Fig.1c), and rises to 0.89 for the last case (Fig. 1d), showing that it is necessary to take
185 all of these three indicators into account.
186 From a statistical point of view, the threshold chosen for a test of significance is defined
187 by the Student law, for 33 samples and a 97.5% confidence interval. This test, applied to
188 the chloride content coefficient, showed that the ratio of the coefficients, *c*, to their
189 standard-deviations σ_c, calculated by the multi-regression (3-parameters), had to remain

above the threshold 2.037.

With this approach for each ND method, the coefficients of the regression were assessed as a function of porosity, saturation rate, and chloride content. For all the EM ND techniques, values depended on the chloride contents assessed at different depths (5, 10, 15, 20 mm and average). Table 2 summarizes the values obtained in the test of significance. The results confirm that all the EM ND techniques are sufficiently sensitive and reliable as far as the estimation of the chloride content is concerned. We note that the highest values (in bold in the table) are obtained when the depth of the estimation of the chloride content tends to the coupled volume of the ND technique.

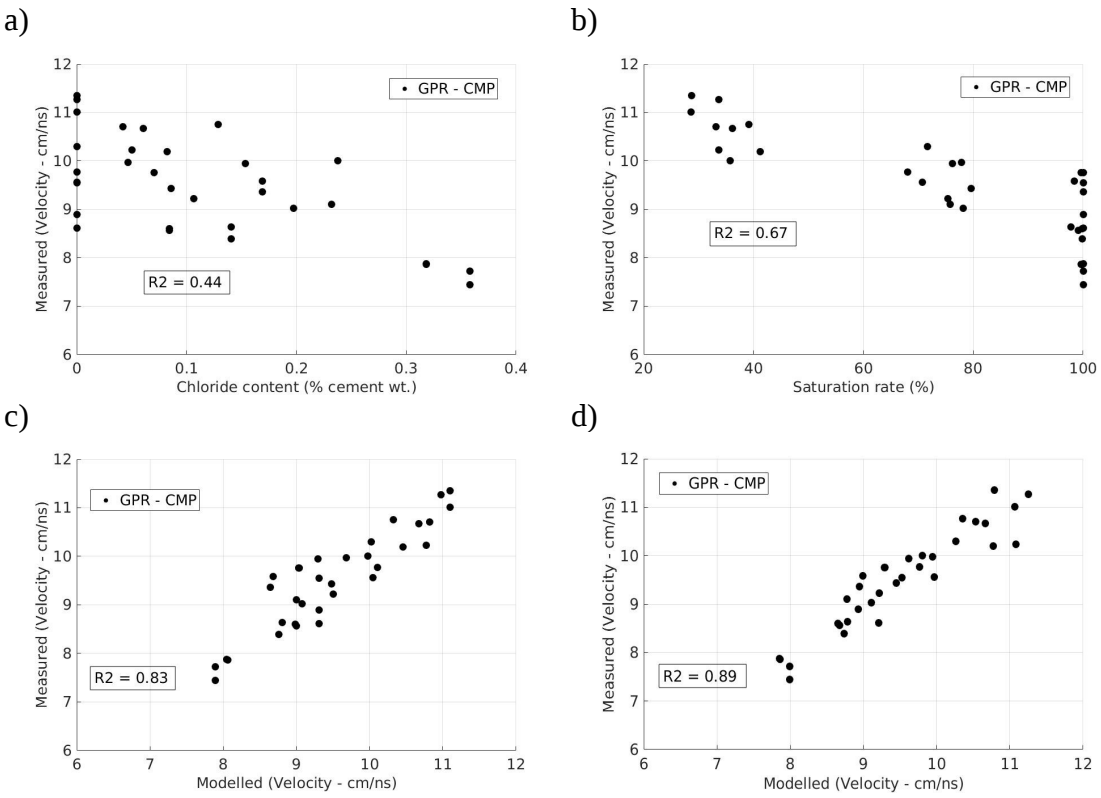

Fig. 1. *GPR velocity measurements, obtained by CMP, as a function of a) the chloride content, b) the saturation rate, c) the GPR velocity modelled using the 2-parameter regression (S_r and Cl^-), d) the GPR velocity modelled using the 3-parameter regression (S_r, Cl^-, Poro)*

Table 3 shows the regression coefficients obtained by keeping the case (depth for estimation of chloride content) leading to the best value in the test of significance, for

each technique.

The values of the coefficients of the indicators, corresponding to Equation 1 and presented in Table 3, enable the ND measurements to be linked to the modelled ones. Some examples of modelling (one per technique) are shown in Figure 2. Their coefficients of determination (R^2) vary from 0.67 for the GPR (Time Offset-L parameter observable) to 0.78 for the capacitive technique (LE), values which increase to above 0.8 when removing one apparent outlier. These results show that, even if the chloride contents are not perfectly constant versus depth in the mixes, the multi-linear regression remains efficient to estimate Cl^-, while taking S_r and *Poro* into account.

Table 2. *Values obtained in test of significance, applied to the Cl^- coefficient, for the ND techniques according to the chosen total chloride content (at 5, 10, 15 and 20 mm and average)*

		Test of significance values (> 2.037)				
	Technique	**Total chloride at 5 mm**	**Total chloride at 10 mm**	**Total chloride at 15 mm**	**Total chloride at 20 mm**	**Total chloride average**
Resistivity	**Q5**	5.25	5.04	5.03	**5.33**	**5.34**
	Q10	4.31	4.10	4.23	**4.53**	**4.41**
Capacitive	**AE**	5.75	**5.85**	5.47	5.43	**5.85**
	LE	6.22	6.31	6.08	**6.38**	**6.51**
GPR	**Epsilon**	3.50	4.44	5.24	**5.66**	4.64
	Velocity	3.66	4.47	4.99	**5.28**	4.59
	Log(peak-to-peak)	5.90	6.27	6.47	**7.30**	6.68
	Ampl CMP	3.83	4.55	5.17	**5.67**	4.80
	Ampl Offset-L	6.75	6.96	6.95	**7.13**	**7.26**
	Time Offset-L	3.15	3.24	3.35	**3.59**	3.39

It is interesting to note that Hugenschmidt and Loser [8] obtained very similar values, about 0.81 for the GPR attenuation (in logarithmic units), versus Cl^-, using air-coupled 2 GHz echoes on concretes containing chlorides. These values are close to our coefficient of 0.77 for Cl^- for the GPR log (peak-to-peak) observable. Sbartaï & al. [23] also found

similar results, with a value of about 0.74, for the coefficient related to Cl^-, using ground-coupled GPR antennas at 1.5 GHz and a normalized reflected echo (in logarithmic units), on homogeneous concrete slabs having 14-15 % porosity. This means that several distinct and independent studies have led to the same reliability for attenuation versus chloride content. This may be considered as a classical dependency. Nevertheless, there is no discussion of uncertainties in these papers.

Table 3. *Coefficient of the multi-regressions of the ND techniques performed in their optimal configuration of chloride content (correponding to the greatest* a/σ_a*)*

		Coefficients					
	Techniques	**Coef. *a* for *Poro***	**Coef. *b* for S_r**	**Coef. *c* for Cl^-**	**Coef. *d***	**R^2**	**Chloride content**
Resistivity	**Q5**	-0.167	-0.0083	-3.574	5.993	0.76	Average
	Q10	-0.157	-0.0079	-3.383	5.637	0.73	20 mm
Capacitive	**AE**	1.037	0.0739	33.30	-8.559	0.72	10 mm
	LE	0.612	0.0757	28.92	-3.527	0.78	Average
GPR	**Epsilon**	0.246	0.0519	9.628	1.600	0.85	20 mm
	Velocity	-0.105	-0.026	-3.397	13.45	0.89	20 mm
	Log(peak-to-peak)	-0.0125	-0.0007	-0.763	-0.077	0.77	20 mm
	Ampl CMP	-0.0015	-0.0003	-0.105	-0.0189	0.73	20 mm
	Ampl Off.-L	-0.0070	-0.0009	-0.227	0.308	0.87	Average
	Time Off.-L	0.0181	0.00235	0.5245	0.788	0.67	20 mm

The influence of chlorides on electrical resistivity is complex since the interstitial fluids in concrete are naturally conductive. Fluid in concrete depends on the composition of the cement and additions, so it is influenced by alkali content: the more alkali there is in the pore water, the smaller is the influence of external fluid [21]. The real value for *Rw* in the Archie's law is a composition of conductance of fluids from the concrete and from external ingresses [24]. Numerous works present the relationship between

electrical resistivity and chloride diffusivity [25-27]. The Nernst-Einstein relationship, used to describe chloride ingress in concrete structure, could be simplified by taking the ideal hypothesis of a constant value for the ion diffusivity, which would give:

$$c_i = k \cdot \left(\frac{1}{R}\right) \quad (4)$$

with c_i the concentration of ion i in the pore water; k a constant deduced from the Nernst-Einstein relationship and associated with the gas constant, the absolute temperature, the ionic valence, the Faraday constant, the ion transport number, and its activity coefficient; and R the electrical resistivity. Apart from ideal cases, the complexity of interactions between concrete interstitial fluid and chlorides may explain why there is no report on the electrical resistivity of concrete versus chloride content of pore water.

To avoid any influence of the ranges of variation for indicators and measurement on the coefficients of the laws, a supplementary step was performed in this study through the normalization (from 0 to 1) of the ND measurements and the indicator values, in the range of their respective values. This allows the techniques and the coefficients to be compared amongst themselves. Concerning the three indicators, their ranges are the following: [0-~0.36% of dry concrete mass] for Cl^-, [28-100%] for S_r and [12.5-18.1%] for *Poro*.

In Table 4, while focusing on the indicators, the chloride content coefficient presents the highest values for all the EM techniques, except for the “Time Offset-Large” observable. The ND approaches, focused on the attenuation of the radar wave, the capacitive and the resistivity techniques, remain the most sensitive to chloride content, the “GPR log (peak-to-peak)” observable being twice as sensitive as the others.

Concerning the saturation rate, the ND techniques devoted to time or velocity of radar

wave propagation are the most sensitive, slightly more than for the chloride content. The difference between the capacitive technique and the GPR time or velocity can be explained by the fact that the EM characteristics of civil engineering materials at the frequencies used (very low GPR frequency band) are sensitive to both chloride and water content [28], due to the predominant effect of interfacial polarization.

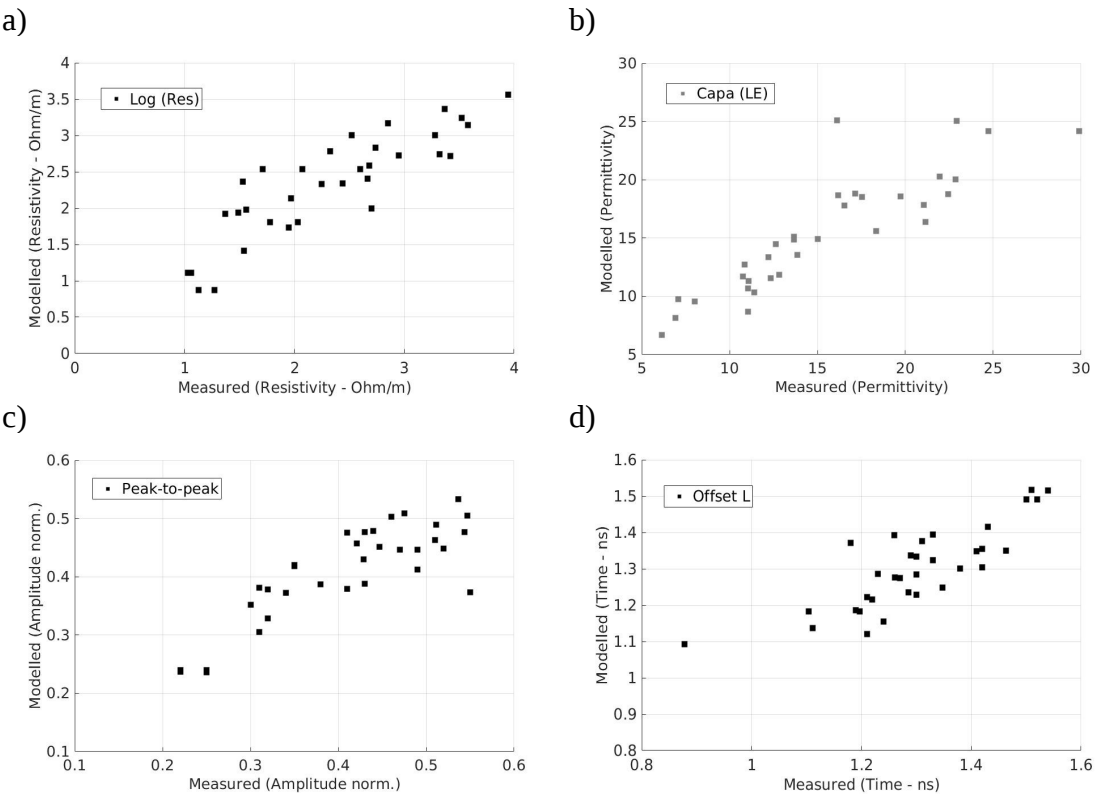

Fig. 2. *Comparison of the measured and calculated observables for a) the resistivity technique – quadripole 5 cm b) the capacitive technique – large electrodes, c) the GPR Log(peak-to-peak) amplitude, d) the GPR amplitude (large offset), at their optimal configuration*

Table 4. *Coefficient of the multi-regressions of the ND normalized measurements performed in their optimal configuration of chloride content (corresponding to the greatest* a/σ_a*)*

	Coefficients obtained with normalized observables and indicators			
Techniques	**Coef. *a* for *Poro***	**Coef. *b* for S_r**	**Coef. *c* for Cl^-**	**Chloride content**

Resistivity	**Q5**	-0.32	-0.20	-0.45	Average
	Q10	-0.35	-0.23	-0.48	20 mm
Capacitive	**AE**	0.18	0.17	0.38	10 mm
	LE	0.14	0.23	0.45	Average
GPR	**Epsilon**	0.15	0.4	0.37	20 mm
	Velocity	-0.15	-0.48	-0.31	20 mm
	Log(peak-to-peak)	-0.18	-0.12	-0.69	20 mm
	Ampl CMP	-0.11	-0.25	-0.49	20 mm
	Ampl Off.-L	-0.23	-0.39	-0.49	Average
	Time Off.-L	-0.20	-0.39	0.28	20 mm

Finally, for the porosity estimation, the electrical techniques give the best performance. This can be explained by the increase in connectivity of pores as the porosity increases, which facilitates ionic displacement and thus the electric current, especially for saturation degrees higher than 40%.

This normalized study thus shows that all these EM techniques are capable of providing information on the following indicators: chloride content, saturation rate and porosity, in concrete mixes. Their sensitivity to these indicators encourages complementary use of these ND techniques if we want to dissociate the indicators surveyed.

4. On-site implementation and discussion

The objective of the campaign described here is to estimate the uncertainty on the values of indicators from ND measurements made at a real site in a tidal zone, using the regressions studied above and the corresponding uncertainties (from the ND measurement and from the regression). Given their high sensitivity to chlorides, three techniques were considered for comparison, out of the three NDT families: resistivity, capacity and GPR. By performing statistical calculations, this study, described below, will quantify the influence of the ND measurements or the regressions on indicator

estimation, from a structural engineering point of view. As the calibration was not performed on the structure in question, only the uncertainties will be studied, and not the absolute values, for which no reliability estimate can be made.

4.1. Presentation of the site

The chosen test site was a 15-year-old reinforced concrete wharf at the port of Saint-Nazaire (France). A large ND campaign was carried out on the site in the framework of the SENSO project, in which all the authors participated. The wharf, the ND techniques, and the destructive analysis are accurately described in [15] and EM values in [29].

The structure tested was a precast reinforced concrete beam exposed to chloride ingress in a tidal zone. The concrete mix used a CEM II/A 32.5PM cement with a water-to-cement ratio of 0.46, and included fly ash and siliceous aggregates as components. The standard tests showed a 28-day compressive strength of about 36 MPa. Gas permeability measurements on five cores gave values corresponding to a porosity in the 11-12% range, and chloride profiles were also obtained from these cores.

The chloride profiles, presented in [15], show values of total chlorides per weight of dry concrete of about 0.025% in the first 5 mm, a maximum of 0.09+/-0.01% at 15+/-2 mm and then a linear decrease to 0.03% at about 32 mm.

Table 5. *ND measurements performed on a concrete wharf at Saint-Nazaire (FR): averaged values and standard deviation per line between brackets*

		Res Q5	Capa LE	GPR velocity	GPR Ampl off L
Internal side	**Line 1**	3.52 (0.399)	5.97 (0.374)	11.53 (0.163)	0.51 (0.0316)
	Line 2	3.41 (0.366)	6.21 (0.384)	11.46 (0.217)	0.51 (0.0263)
	Line 3	3.35 (0.283)	6.25 (0.369)	11.47 (0.224)	0.50 (0.0218)
External side	**Line 1**	3.36 (0.323)	6.91 (0.133)	11.05 (0.282)	0.45 (0.0182)
	Line 2	3.41 (0.365)	6.95 (0.254)	10.94 (0.271)	0.44 (0.0286)
	Line 3	3.45 (0.431)	6.94 (0.189)	11.04 (0.246)	0.45 (0.0203)

NDT method S.D	0.012	0.0003	0.003	0.0055

ND measurements were performed on each side of the beam – the external side exposed to wind, rain and ocean spray, and the protected, internal side under the wharf deck – on three horizontal lines. Thirty measurements were recorded per face, at the centre of the reinforcement meshes. The ND values shown in Table 5 are the average of each line. An ND procedure repeated several times at one point (centre of a reinforced mesh) in order to find the standard deviation (S.D.) of each NDT method on the structure (last line of table 5).

4.2. Methodological approach

Non-destructive measurements led to the determination of the observables, from which the indicators were deduced through the inverse analysis of a specific relationship for each technique, for instance Eq.1. During this process, uncertainty appeared at various levels, mainly (Table 6 based on Eq.1):

- on the measurement (uncertainty on observable). This uncertainty was assessed during the investigation of the structure by repeated measurements. For this study, the measurement uncertainty is the standard deviation of repeated measurements relative to the average value (in other words the Coefficient of Variation CoV), given in terms of relative uncertainty;
- on the relationship between observable and indicator (model error). This error is linked to the reliability of the calibration process. In this study, it corresponds to the standard error value of the parameter considered, as assessed during the linear regression calculation relative to the average value of the parameter (the CoV).

The sensitivity analysis showing the effect of these various uncertainty levels on diagnostic reliability is performed through a Monte Carlo simulation. It consists of performing repeated sampling for a parameter described by its statistics (average and CoV). The simulated population respects the same statistical distribution. Then from each "simulated uncertain term" of the population, it is possible assess the uncertainty propagating to the final result. For this study, and at each step, 1000 values were simulated. According to the objective, the uncertainties could be simulated on different parameters.

Table 6. *Uncertainty levels on Eq.1*

parameter	**for instance in Eq.1**	**Symbol**	**uncertainty**	**uncertainty level**
Observable	Velocity GPR	V_{GPR}	+/- δV_{GPR}	measurement
law	Porosity coefficient	a	+/- δa	calibration
law	Saturation coefficient	b	+/- δb	calibration
law	Chloride content coefficient	c	+/- δc	calibration
law	Constant coefficient	d	+/- δd	calibration
indicator	Porosity	$Poro$	+/- $\delta Poro$	interpretation
indicator	Saturation rate	Sr	+/- δSr	interpretation
indicator	Chloride content	Cl^-	+/- δCl^-	interpretation

If the measurement uncertainty is considered, with the perfect regression model, δV_{GPR} exists, and δa, δb, δc, δd are equal to 0. Respectively one thousand "measured" values are considered (statistically correct), leading to the calculation of a thousand values for $Poro$, Sr and Cl^- after inversion. Thus the average values can be assessed for each indicator as well as $\delta Poro$, δSr, and δCl^-. If the measurement is considered as perfect and the uncertainty is only on the regression model, δV_{GPR} equals 0, and δa, δb, δc, δd exist. From measurements, and considering the thousand values each for a, b, c and d (for the observable under consideration) to be statistically correct, a thousand values for

poro, Sr and Cl^- are assessed by inversion. Here again, average values are assessed for indicators and for $\delta Poro$, δSr, and δCl^-. Then, both approaches are studied and the uncertainties on *Poro*, S_r and Cl^- are compared.

Moreover, the inversion process is carried out considering matrix calculations (Eqs 5 to 7) with *O* the matrix of observables, *d* the matrix containing the constant term of each regression, *I* the matrix of indicators, and *M* the matrix of regression coefficients. Inversion consists to of determining the matrix $[M]^{-1}$, inverse of [*M*], thus leading to the assessment of its determinant: Det(*M*).

$$[O]-[d]=[I]x[M] \tag{5}$$

with

$$\begin{bmatrix} obs1 \\ obs2 \\ obs3 \end{bmatrix} - \begin{bmatrix} d1 \\ d2 \\ d3 \end{bmatrix} = \begin{bmatrix} indic1 \\ indic2 \\ indic3 \end{bmatrix} \cdot \begin{bmatrix} a1 & b1 & c1 \\ a2 & b2 & c2 \\ a3 & b3 & c3 \end{bmatrix} \tag{6}$$

Inversion consists of assessing $[M]^{-1}$ in order to solve the following equation:

$$[I]=([O]-[d])x[M]^{-1} \tag{7}$$

This problem is not solvable if Det(*M*) is equal to 0, which would correspond to the situation where the models have the same coefficients of regression. In this case, no additional information would be provided by any NDT method compared with the others. If Det(M) is very close to 0, the calculation error will be very high. To overcome this difficulty it is decided to consider uncertainties of indicators, namely $\delta Poro$, δSr, and δCl^- instead of the indicators themselves.

4.3. Influence of types of uncertainty of NDT methods

For this study, we considered the triplet: resistivity Q5, capa LE, and GPR velocity,

chosen as the three techniques presenting the best relationship to chloride content in each of the three NDT families (see R^2 values in Table 3).

An overview of the results is given in the following tables (7, 8 and 9). Case 1 corresponds to ND values associated with their average standard deviation per line, which includes a part of the material variability along the beam. Case 2 corresponds to the standard deviation calculated at a measurement point, which corresponds to the technique variability. Standard deviations decrease from roughly 40, 28, 23 and 2.4% in case 1 to 1.2, 0.03, 0.3 and 0.55% in case 2 for res_Q5, capa_LE, GPR velocity and GPR_Ampl_off_L, respectively.

The first observations in Tables 7 and 8 show that uncertainties on the regression models lead to an unacceptable estimation of indicators. The models obtained from laboratory experiments, which were not suited to Saint Nazaire wharf, are used. This is made obvious by the negative values for chloride factors. So, the influence of model error or measurement uncertainty is estimated by the error of indicator assessment and not to by the value of the indicator. This implies that a calibration of the regression models is necessary for each ND technique for every ND inspection on a new concrete structure.

Table 7. *Statistical inversions of the ND measurements, performed on a concrete wharf (Table 5), under the hypothesis of perfect regression models or perfect measurements and considering Case 1*

		Perfect models (uncert. on meas.)			**Perfect measurements (uncert. on models)**		
Case 1		**Porosity**	**Sat**	**Cl-**	**Porosity**	**Sat**	**Cl-**
Int. side	**L1**	14.3 (**29%**)	19.1 (**65.3%**)	-0.025(**306%**)	19.2 (**447%**)	20.3 (**768%**)	-0.17 (**1569%**)
	L2	15.2 (**26.2%**)	19.7 (**76.1%**)	-0.036 (**217%**)	20.4 (**447%**)	21.2 (**773%**)	-0.19 (**1460%**)
	L3	15.9 (**19.1%**)	18.1 (**79.2%**)	-0.046 (**143%**)	21.2 (**94.4%**)	19.1 (**882%**)	-0.21 (**1426%**)
Ext. side	**L1**	15.2 (**24.1%**)	17.4 (**46%**)	-0.060 (**127%**)	20.2 (**433%**)	42.2 (**388%**)	-0.22 (**1257%**)
	L2	14.7 (**27.2%**)	17.4 (**37.6%**)	-0.070 (**114%**)	19.5 (**429%**)	50.0 (**321%**)	-0.22 (**1198%**)

	L3	14.0 (**33.3%**)	16.8 (**40.4%**)	0.044 (**198%**)	18.7 (**433%**)	44.5 (**349%**)	-0.19 (**1351%**)

As inversions show similar results for the internal and the external sides, only the values of the internal face are presented below.

Table 8. *Statistical inversions of the ND measurements, performed on the internal side of the concrete wharf (Table 5), under the hypothesis of perfect regression models or perfect measurements and considering Case 2*

Internal side		**Perfect models (uncert. on meas.)**			**Perfect measurements (uncert. on models)**		
		Porosity	**Sat**	**Cl-**	**Porosity**	**Sat**	**Cl-**
Case 2	**L1**	14.4 (**0.9%**)	18.6 (**1.6%**)	-0.026 (**8.3%**)	19.2 (**447%**)	20.3 (**768%**)	-0.17 (**1569%**)
	L2	15.3 (**0.8%**)	19.4 (**1.6%**)	-0.038 (**5.5%**)	20.4 (**447%**)	21.2 (**773%**)	-0.19 (**1460%**)
	L3	15.9 (**0.8%**)	17.4 (**1.7%**)	-0.044 (**4.7%**)	21.2 (**94.4%**)	19.1 (**882%**)	-0.21 (**1426%**)

The analysis of Table 7 is mainly focused on the uncertainty values (percentage in bold characters in brackets), and not on the values themselves, since the regression models are not created on the surveyed concrete but on laboratory slabs. The first findings show extremely high levels for $\delta Poro$, δSr, and δCl^- in the case of uncertainty of models, in a range ten times above those for the case of uncertainty of measurements.

The second point concerns the comparison of cases 1 and 2 when considering perfect models. We can note similar values of indicators but a large difference in the uncertainty values. Taking account of the variability of ND measurements from a large zone (Case 1) on the inversion induces results that are unacceptable because unreliable. We must consider only the uncertainty of the NDT on this concrete mix (obtained from the repetitive procedure on one representative local zone) rather than the integrated uncertainty combining NDT and the variability of the material.

Finally, from a structural engineering point of view, the uncertainties on the indicators

Poro, *Sr*, and Cl^- give rise to acceptable ranges when the hypothesis of perfect regression models is maintained (if they can be designed on the concrete being surveyed) and when the standard deviation of each ND technique is found on site.

4.4. Influence of combination of observables

The choice of the three techniques also has an influence on uncertainties of assessment. We compare the results obtained when the techniques were selected on their own reliability with respect to chloride variations (as in Section 3, techniques chosen on the R^2 value, see Table 3), or if the techniques were chosen according to their complementarity (based on the assessment of the highest determinant value, see Eqs. 5 to 7).

The two cases are studied in Table 9, which shows the influence of observable combination on the assessment of indicators. As expected, when the value of Det(*M*) decreases too much, the inversion process induces unacceptable uncertainties, as seen for the triplet Techn. Res (Q5) / Capa (LE) / GPR ampl.

Table 9. *Statistical inversions of the ND measurements, performed on the internal side of the concrete wharf (Table 5), including either the GPR velocity or the GPR amplitude*

Perfect models (uncert. on meas.)		**Porosity**	**Sat**	**Cl-**
Techn. Res / Capa / **GPR vel.**	**Line 1**	14.4 (**0.9%**)	18.6 (**1.6%**)	-0.026 (**8.3%**)
Average S.D. per line	**Line 2**	15.3 (**0.8%**)	19.4 (**1.6%**)	-0.038 (**5.5%**)
Det = -0.0464	**Line 3**	15.9 (**0.8%**)	17.4 (**1.7%**)	-0.044 (**4.7%**)
Techn. Res / Capa / **GPR ampl. Off. L**	**Line 1**	4.7 (**4.5%**)	-849 (**1.9%**)	2.45 (**1.8%**)
	Line 2	4.2 (**5.0%**)	-965 (**1.6%**)	2.77 (**1.6%**)
Average S.D. per line	**Line 3**	3.0 (**6.9%**)	-1129 (**5.9%**)	3.23 (**1.3%**)
Det = -0.00092				

An explanation can be furnished by Figure 3, which shows the regression relations for the two distinct NDT triplets (from Table 9) while focusing on chloride. Ideally, the estimation of chloride content should be made by the intersection of the three regressions. In both cases, there is no single intersection of the three curves. Nevertheless, the uncertainty of the apparent solution (not exact since the calibration does not correspond to the material under study) is represented by the band covered by the three ranges of uncertainty for each of the observables.

The bandwidth of uncertainty on chloride content varies from less than 0.3 for the first case (blue arrow in Fig. 3a), to more than 0.35 for the second case (blue arrow in Fig. 3b). The closer the three regressions intersect (the farther the determinant from Eq. 7 is from 0) the less uncertainty there is. Then, for the second case, it is shown that both resistivity and GPR amplitude have similar sensitivities to chloride (expressed by a determinant very close to 0), and the third technique does not significantly improve the assessment of indicator. For these two cases DET are -0.0464, and -0.0009, respectively.

a) b)

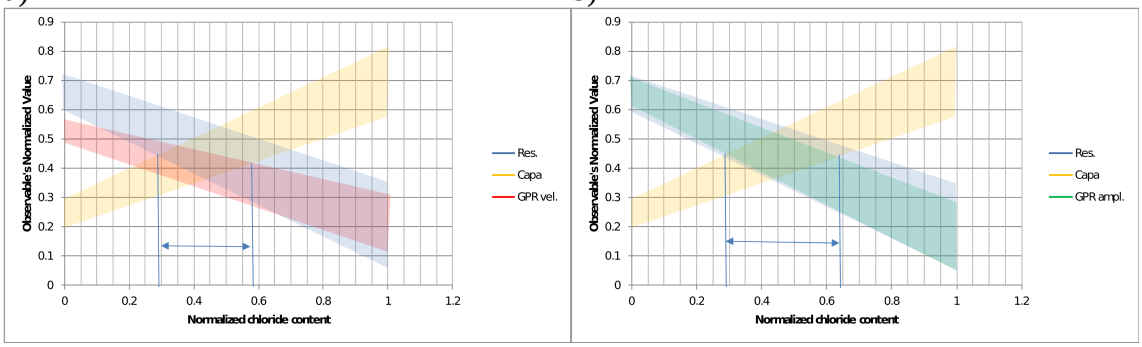

Fig. 3. *Regressions of selected ND techniques (normalized values) versus chloride content for the triplets a) Techn. Res (Q5) / Capa (LE) / GPR velocity and b) Techn. Res (Q5) / Capa (LE) / GPR ampl. The bandwidths correspond to the uncertainties of each regression.*

4.5. Discussion on how to choose an ideal third ND technique

The question of the choice of three complementary techniques could be then based on the determinant value. To test this approach, and having already chosen the resistivity and capacitive techniques, a third NDT is chosen: GPR epsilon, which leads to Det(*M*) = 0.0721. The estimation of chloride content uncertainty with this new triplet (Fig. 4a) is 0.35. This value is in the range of the first results, proving that this approach is not sufficient when working with EM techniques.

Going further in this study, we also tested this criterion by considering an ideal virtual technique fairly perpendicular to the first two (Fig. 4b). The uncertainty level of this technique was taken to be in the same range as the others. The result shows a chloride content uncertainty decreasing to 0.15. Finally, it should be noted that the uncertainty of the ideal ND technique could strongly influence the uncertainty on indicators, even if the intersection is quite perpendicular (that is to say, even if the determinant is high).

a) b)

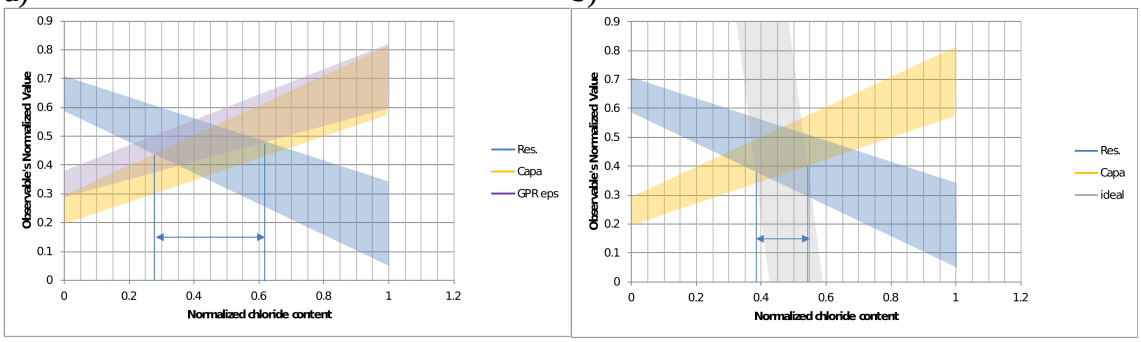

Fig. 4. *Regressions of selected ND techniques (normalized values) versus chloride content for the triplets a) Techn. Res (Q5) / Capa (LE) / GPR eps and b) Techn. Res (Q5) / Capa (LE) / ideal techn. The bandwidths correspond to the uncertainties of each regression.*

5. Conclusion

The results presented in this paper concern the implementation of different NDT methods (using radar, capacitive and resistivity techniques) for the detection of

chlorides in concrete. Three different concrete mixes were tested in the laboratory with different levels of saturation and involving two concentrations of NaCl. A multi-linear regression, depending on the three indicators: chloride content, saturation rate and porosity, was performed for each ND technique, under the hypothesis of averaged indicator values without a depth gradient.

The results show that all the techniques devoted to attenuation measurements or the resistivity are very sensitive to the presence of chlorides. This phenomenon is less visible for the relative permittivity, as the frequency increases in the GPR frequency band. Concerning the other two indicators, more than half of the ND techniques are less than half as sensitive to them as to the chloride content.

Experiments on a real site in a marine environment have shown that it is necessary to take two other indicators into account: the saturation rate and the porosity, to properly estimate the chloride content through a multi-linear regression approach. A statistical study was performed on the influence of the accuracy of ND measurements and the model error on chloride content, from a structural engineering point of view.

The principal results show that:

- all the ND techniques must be calibrated on the structure actually surveyed,
- the combination of 3 techniques sensitive to chloride is not necessarily the best ND triplet,
- the determinant of the regression equations considered as an indicator of reliability (for chloride estimation), is not sufficient because it is sensitive to the 3 techniques,
- when considering a virtual ideal technique (the regression slope of which would be “perpendicular” to those of the other techniques), the parametric study shows the importance of the uncertainty of each technique in the estimation of the chloride

content.

Finally, it is illusory to believe that it is possible to accurately estimate the chloride content of a concrete structure using the hypothesis that all other indicators are spatially constant. The paper has highlighted the present limitations of the various possible approaches for chloride content assessment.

Acknowledgments

The French National Research Agency (ANR) is gratefully acknowledged for supporting the ANR-PGCU SENSO project. This work is a contribution to COST action TU1208 on “Civil engineering applications of GPR”.

Our thanks are extended to Susan Becker, a native English speaker, commissioned to proofread the final English version of this paper.

Glossary

Chloride content: ratio (percentage) of the weight of total chloride (free and bound) to the weight of dry concrete.

Durability indicator: property describing the concrete in term of durability and performances (i.e. porosity, density, resistance, Young modulus, chloride content, moisture...).

Indicator: generic term designating all durability indicators and more generally all the properties involved in concrete durability

Multi-linear regression: approach of modeling the relationship between a dependent variable (i.e. permittivity) and few conditioning variables (i.e. chloride content, porosity...) using linear mathematical expression.

ND observable: direct value (i.e. permittivity, resistivity...) or extracted value (i.e. wave attenuation or velocity…) from non-destructive (ND) measurements.

Porosity: ratio (in percentage) of the volume of void to the total volume of material.

Saturation rate: ratio (in percentage) of a volume of fluid (interstitial solution for concrete) to the total volume of voids inside concrete.

uncertainty: statistical expression of the dispersion of a result, associated to the imperfect and/or unknown information. For an inverse process to predict a value (ie. Chloride content), it can result from both imperfect measurement and imperfect model.

Variability: expression characterizing the effect of the natural unmastered variations of the material properties at the measurement scale. It leads to the dispersion of the measurement results which can be attributed to the object (material) being measured.

References

[1] Baroghel-Bouny V, Belin P, Maultzsch M, Henry D. AgNO3 spray tests - Advantages, weaknesses, and various applications to quantify chloride ingress into concrete. Part 1: Non-steady-state diffusion tests in laboratory and exposure to natural conditions. Mater Struct 2007;40:759-781.

[2] Tutti K. Corrosion of steel in Concrete. Research Report 4.82. Swed Cem Concr Res Inst, Stockholm (SE), 1982.

[3] Kropp J, Alexander M. Non-destructive methods to measure ion migration. In: RILEM Report 040 Non-destructive evaluation of the penetrability and thickness of concrete cover. RILEM TC 189-NEC: State of the art report 2007;13-34.

[4] M. Torres-Luque M, Bastidas-Arteaga E, Schoefs F, Sánchez-Silva M, Osma JF. Non-destructive methods for measuring chloride ingress into concrete: State-of-

544 the-art and future challenges. Constr Build Mater 2014;68:68-81.
545 **[5]** Soutsos MN, Bungey JH, Millard SG, Shaw MR, Patterson A. Dielectric
546 properties of concrete and their influence on radar testing. NDT&E Int
547 2001;34(6):419-25.
548 **[6]** Laurens S, Balayssac JP, Rhazi J, Arliguie G. Influence of concrete moisture
549 upon radar waveform. Mater Struct 2002;35(248):198–203.
550 **[7]** Klysz G, Balayssac JP. Determination of volumetric water content of concrete
551 using ground-penetrating radar. Cem Concr Res 2007;37(8):1164-71.
552 **[8]** Hugenschmidt J, Loser R. Detection of chlorides and moisture in concrete
553 structures with ground penetrating radar. Mater Struct 2008;41(4):785–92.
554 **[9]** Kalogeropoulos A, Van der Kruk J, Hugenschmidt J, Busch S, Merz K.
555 Chlorides and moisture assessment in concrete by GPR full waveform inversion.
556 Near Surf Geophys 2011;9(3):277-86.
557 **[10]** Villain G, Ihamouten A, du Plooy R, Palma Lopes S, Dérobert X. Use of
558 electromagnetic non-destructive techniques for monitoring water and chloride
559 ingress into concrete. Near Surf Geophys 2015;13:299-309.
560 **[11]** Loche JM, Lataste JF, Amiri O, Larget M, Tahlaiti M, Aït-Mokhtar A.
561 Evaluation of cover concrete and assessment of chloride ingress into cover concrete
562 by Non Destructive Testing. Part.I - Samples preparation - Porosity and resistivity
563 measurements. 1st Int Conf MEDACHS´08 Proc, Lisbon (PT), 2008.
564 **[12]** Dérobert X, Lataste JF, Loche JM, Villain G, Larget M, Aït-Mokhtar A, Amiri
565 O, Coffec O, Tahlaiti M, Durand O, Lu L, Abraham O. Evaluation of cover concrete
566 and assessment of chloride ingress into cover concrete by Non Destructive
567 Techniques. Part II – Comparison of NDT measurements and correlations. 1st Int

Conf MEDACHS´08 Proc, Lisbon (PT), 2008.

[13] Balayssac JP, Laurens S, Arliguie G, Breysse D, Garnier V, Dérobert X, Piwakowski B. Description of the general outlines of the French project SENSO – Quality assessment and limits of different NDT methods. Constr Build Mater 2012;35:131–8.

[14] Ploix MA, Garnier V, Breysse D, Moysan J. NDE data fusion to improve the evaluation of concrete structures. NDT&E Int 2011;44(5):442-8,doi:10.1016/j.ndteint.2011.04.006.

[15] Sbartaï ZM, Breysse D, Larget M, Balayssac JP. Combining NDT Techniques for Improving Concrete Properties Evaluation. Cem & Conc Comp, 2012;34(6):725-33.

[16] Villain G, Sbartaï ZM, Dérobert X, Garnier V, Balayssac JP. Durability diagnosis of a concrete structure in a tidal zone by combining NDT methods: laboratory tests and case study. Constr Build Mater 2012;37:893–903.

[17] Dérobert X, Iaquinta J, Klysz G, Balayssac JP. Use of capacitive and GPR techniques for non-destructive evaluation of cover concrete. NDT&E Int 2008;41(1):44-52.

[18] Chataigner S, Saussol JL, Dérobert X, Villain G. Temperature influence on electromagnetic measurements of concrete moisture", Eur Journ Env & Civil Eng 2015;19(4):482-95,http://dx.doi.org/10.1080/19648189.2014.960102.

[19] Lataste JF, Sirieix C, Breysse D, Frappa M. Electrical resistivity measurement applied to cracking assessment on reinforced concrete structures in civil engineering. NDT&E Int 2003;36(6):383-94.

[20] Lataste JF, de Larrard T, Benboudjema F, Semenadisse J. Study of electrical

592 resistivity: variability assessment on two concretes: protocol study in laboratory and
593 assessment on site. Eur Journ Env & Civil Eng 2012;16(3-4):298-310.
594 **[21]** Hunkeler F. The resistivity of pore-water solution - a decisive parameter of
595 rebar corrosion and repair methods. Constr Build Mater 1996;10(5):381-9.
596 **[22]** Saleem M, Shameem M, Hussain SE, Maslehuddin M. Effect of moisture,
597 chloride, and sulfate contamination on the electrical resistivity of Portland Cement
598 Concrete. Constr Build Mater 1996;10(3):209-14.
599 **[23]** Sbartaï ZM, Laurens S, Balayssac JP, Arliguie A, Ballivy G. Ability of the
600 direct wave of radar ground-coupled antenna for NDT of concrete structures.
601 NDT&E Int 2006;39:400-7.
602 **[24]** McCarter WJ, Ezirim H, Emerson M. Properties in the cover zone :Water
603 penetration, sorptivity and ionic ingress. Mag Concr Res 1996;48(176):149-56.
604 **[25]** Andrade C, Andrea R, Rebolledo N. Chloride ion penetration in concrete: the
605 reaction factor in the electrical resistivity model. Cem Concr Comp 2014;47:41-6.
606 **[26]** Polder RB, Peelen WHA. Characterisation of chloride transport and
607 reinforcement corrosion in concrete under cyclic wetting and drying by electrical
608 resistivity. Cem Concr Res 2002;24:427-35.
609 **[27]** Sengul O. Used of electrical resistivity as an indicator for durability. Constr
610 Build Mater 2014;73:434-41.
611 **[28]** Dérobert X, Villain G, Cortas R, Chazelas JL. EM characterization of
612 hydraulic concretes in the GPR frequency-band using a quadratic experimental
613 design. 7th Int Symp NDT-CE Proc, Nantes (FR), 2009.
614 **[29]** Balayssac JP, Laurens S, Lataste JF, Dérobert X. Evaluation of chloride
615 contamination in concrete by combining non destructive testing methods. 2nd Int

617

618 **Appendix**

619 ***Table A1.*** *Saturation rate, porosity and total chloride content (by weight of dry concrete) for all*

620 *the concretes*

Sample	N°	Expected Sat. Rate	Porosity (%)	Sat. rate (%)	Total chloride at 5 mm	Total chloride at 10 mm	Total chloride at 15 mm	Total chloride at 20 mm	Total chloride average
G8	1	40	18.1	28.8	0.00	0.00	0.00	0.00	0.00
	2		18.1	33.1	0.08	0.07	0.06	0.04	0.06
	3		18.1	35.7	0.34	0.31	0.25	0.24	0.29
	4	80	18.1	68.1	0.00	0.00	0.00	0.00	0.00
	5		18.1	75.4	0.11	0.11	0.11	0.11	0.11
	6		18.1	75.8	0.26	0.22	0.21	0.23	0.23
	7	100	18.1	100.0	0.00	0.00	0.00	0.00	0.00
	8		18.1	99.1	0.14	0.08	0.07	0.08	0.10
	9		18.1	99.8	0.14	0.08	0.07	0.08	0.10
	10		18.1	99.6	0.39	0.34	0.34	0.32	0.34
	11		18.1	100.0	0.39	0.34	0.34	0.32	0.34
G3	12	40	15.5	28.7	0.00	0.00	0.00	0.00	0.00
	13		15.5	36.2	0.05	0.06	0.06	0.06	0.06
	14		15.5	39.1	0.19	0.16	0.14	0.13	0.15
	15	80	15.5	70.7	0.00	0.00	0.00	0.00	0.00
	16		15.5	79.6	0.24	0.10	0.06	0.09	0.12
	17		15.5	78.1	0.46	0.27	0.23	0.20	0.29
	18	100	15.5	100.0	0.00	0.00	0.00	0.00	0.00
	19		15.5	97.8	0.21	0.20	0.18	0.14	0.18
	20		15.5	99.8	0.21	0.20	0.18	0.14	0.18
	21		15.5	100.0	0.42	0.35	0.35	0.36	0.37
	22		15.5	100.0	0.42	0.35	0.35	0.36	0.37
G1	23	40	12.5	33.6	0.00	0.00	0.00	0.00	0.00
	24		12.5	33.7	0.10	0.07	0.06	0.05	0.07
	25		12.5	41.2	0.16	0.14	0.09	0.08	0.12
	26	80	12.5	71.7	0.00	0.00	0.00	0.00	0.00
	27		12.5	77.8	0.06	0.06	0.05	0.05	0.05
	28		12.5	76.2	0.18	0.13	0.17	0.15	0.16
	29	100	12.5	100.0	0.00	0.00	0.00	0.00	0.00
	30		12.5	100.0	0.17	0.12	0.08	0.07	0.11
	32		12.5	99.6	0.17	0.12	0.08	0.07	0.11
	32		12.5	100.0	0.37	0.25	0.19	0.17	0.25
	33		12.5	98.4	0.37	0.25	0.19	0.17	0.25

Table A2. *ND measurements*

Sample	N°	Capa (LE) (-)	Capa (ME) (-)	Log (Res – 5 cm) (Ω.m)	Log (Res – 10 cm) (Ω.m)	GPR velocity (cm/ns)	GPR pic-pic (-)	Log(GPR att.) (-)	GPR Ampl (D4) - (-)	GPR OD (D4) (ns)
G8	1	7.07	7.34	3.32	2.97	11.35	0.543	-0.054	0.154	1.104
	2	12.82	16.34	2.60	2.73	10.71	0.520	-0.055	0.165	1.220
	3	17.53	22.64	1.95	1.94	10.00	0.320	-0.066	0.100	1.330
	4	10.84	12.31	2.67	2.35	9.77	0.447	-0.063	0.115	1.261
	5	21.14	24.11	1.37	1.36	9.23	0.310	-0.077	0.071	1.410
	6	22.86	25.36	1.54	1.56	9.11	0.310	-0.095	0.045	1.430
	7	13.67	15.50	1.97	1.80	8.89	0.429	-0.065	0.104	1.463
	8	16.53	19.44	2.03	2.10	8.57	0.410	-0.084	0.052	1.260
	9	21.05	23.44	1.78	1.78	8.60	0.320	-0.084	0.049	1.330
	10	22.93	37.65	1.13	1.16	7.87	0.220	-0.088	0.028	1.540
	11	16.12	17.26	1.27	1.17	7.88	0.250	-0.105	0.023	1.510
G3	12	6.92	7.52	3.58	3.25	11.01	0.547	-0.058	0.181	1.112
	13	11.39	13.15	2.74	2.83	10.67	0.510	-0.053	0.155	1.190
	14	12.20	16.08	1.71	1.72	10.76	0.350	-0.052	0.166	1.300
	15	11.08	12.58	2.32	2.04	9.56	0.430	-0.071	0.142	1.285
	16	18.34	21.68	1.53	1.52	9.43	0.350	-0.073	0.082	1.380
	17	21.95	23.29	1.49	1.35	9.03	0.300	-0.080-	0.056	1.420
	18	13.85	16.19	2.07	1.84	8.61	0.421	0.061	0.120	1.420
	19	19.72	19.71	2.70	2.74	8.64	0.550	-0.101	0.041	1.180
	20	22.43	24.34	1.56	1.57	8.39	0.340	-0.092	0.040	1.310
	21	29.90	27.76	1.03	1.03	7.45	0.220	-0.125	0.012	1.520
	22	24.74	23.17	1.06	1.02	7.72	0.250	-0.121	0.017	1.500
G1	23	6.15	5.86	3.94	3.38	11.27	0.537	-0.064	0.158	0.878
	24	11.04	12.38	3.37	3.50	10.23	0.460	-0.060	0.129	1.210
	25	11.04	13.52	2.85	2.82	10.20	0.440	-0.049	0.155	1.240
	26	8.02	7.59	3.52	3.22	10.30	0.475	-0.066	0.166	1.196
	27	12.35	12.96	2.52	2.51	9.97	0.410	-0.059	0.129	1.210
	28	12.62	14.09	2.68	2.64	9.95	0.490	-0.060	0.126	1.270
	29	10.75	11.17	3.28	3.06	9.55	0.511	-0.057	0.155	1.347
	30	15.02	15.85	3.42	3.52	9.76	0.490	-0.067	0.115	1.230
	32	13.65	15.40	2.95	3.01	9.76	0.470	-0.067	0.115	1.300
	32	17.14	17.75	2.25	2.27	9.36	0.380	-0.071	0.079	1.290
	33	16.19	18.62	2.44	2.41	9.58	0.430	-0.070	0.096	1.300